

PAPER • OPEN ACCESS

## Dissipative gravitational bouncer on a vibrating surface

To cite this article: J. S. Espinoza Ortiz and R. E. Lagos 2017 *J. Phys.: Conf. Ser.* **936** 012003

View the [article online](#) for updates and enhancements.

### Recent citations

- [A relativistic bouncer on a vibrating surface](#)  
J. S. Espinoza Ortiz and R. E. Lagos



**IOP | ebooks™**

Bringing you innovative digital publishing with leading voices to create your essential collection of books in STEM research.

Start exploring the [collection](#) - download the first chapter of every title for free.

# Dissipative gravitational bouncer on a vibrating surface

J. S. Espinoza Ortiz<sup>1</sup>, R. E. Lagos<sup>2</sup>

<sup>1</sup>Departamento de Física, UAF, Universidade Federal de Goiás, Catalão, Goiás 75704/020, Brasil.

<sup>2</sup>Departamento de Física, IGCE, UNESP, Rio Claro, São Paulo 13500/970, Brasil.

E-mail: [jsespino@physics.org](mailto:jsespino@physics.org)

**Abstract.** We study the dynamical behavior of a particle flying under the influence of a gravitational field, with dissipation constant  $\lambda$  (Stokes-like), colliding successive times against a rigid surface vibrating harmonically with restitution coefficient  $\alpha$ . We define re-scaled dimensionless dynamical variables, such as the relative particle velocity  $\Omega$  with respect to the surface's velocity; and the real parameter  $\tau$  accounting for the temporal evolution of the system. At the particle-surface contact point and for the  $k'$ th collision, we construct the mapping described by  $(\tau_k, \Omega_k)$  in order to analyze the system's nonlinear dynamical behavior. From the dynamical mapping, the fixed point trajectory is computed and its stability is analyzed. We find the dynamical behavior of the fixed point trajectory to be stable or unstable, depending on the values of the re-scaled vibrating surface amplitude  $\Gamma$ , the restitution coefficient  $\alpha$  and the damping constant  $\lambda$ . Other important dynamical aspects such as the phase space volume and the one cycle vibrating surface (decomposed into absorbing and transmitting regions) are also discussed. Furthermore, the model rescues well known results in the limit  $\lambda = 0$ .

## 1. Introduction

The dynamical behavior of a particle bouncing on a vertically vibrating surface has been extensively studied, both theoretically and experimentally [1, 2, 3]. The model was established as an alternative to the Fermi-Ulam model for the cosmic ray acceleration mechanism introduced by Fermi [4, 5]. A fundamental characteristic of the model lies on its dynamical map exactly iterated at any time, under the assumption that the ball is considered small so the surface is not affected by repeated impacts of the ball. There are different types of ball-particle collision mechanisms to be considered, displaying diverse periodic, non-periodic and chaotic motion regimes. However, most of the map studies assume that the distance traveled by the free falling ball between impacts is large compared to the overall displacement of the vibrating surface, and an approximate equation for the time interval between impacts, is obtained [6]. In this work, we study a model that considers the explicit equation of motion of the ball, as in [7]. In addition, we assume the particle to be under the influence of a Stokes-like damping force. In section 2 we present the dynamical equations governing the particle-surface system, and the mapping is presented in section 3. We compute and discuss the stability of the fixed points in section 4. General aspects related to the dynamics of the system are present in section 5 and the conclusions follow in section 6.



## 2. The bouncer

Let us consider an unitary mass particle flying under the influence of a gravitational field and a Stokes-like damping force. The particle collides repetitive times with a vibrating rigid platform governed by the amplitude  $s(t) = a \sin(\omega t)$ . The nature of the collision is defined by the restitution coefficient  $\alpha$ , a real positive parameter. The particle dynamics is described by Newton's second law:  $\ddot{x}(t) = -\lambda \dot{x}(t) - g$ , recasted, in convenient dimensionless variables, as

$$\ddot{X}(\tau) = -\tilde{\lambda}V(\tau) - 2, \quad (1)$$

where  $t = T\tau$ ,  $x = \frac{g}{2}T^2X$ ,  $\dot{x} = \frac{g}{2}T\dot{X}$ ,  $\ddot{x} = \frac{g}{2}\ddot{X}$  and  $\tilde{\lambda} = \lambda T$  with  $T = \frac{2\pi}{\omega}$ . Also we define  $\Delta\tau = \tau - \tau_o \geq 0$  and integrate the equation with initial conditions  $X(\tau_o)$  and  $V(\tau_o)$ , yielding

$$\begin{aligned} V(\tau) &= -\frac{2}{\tilde{\lambda}} + \left[V(\tau_o) + \frac{2}{\tilde{\lambda}}\right] \exp(-\tilde{\lambda}\Delta\tau), \\ X(\tau) &= X(\tau_o) - \frac{2}{\tilde{\lambda}}\Delta\tau - \frac{1}{\tilde{\lambda}} \left[V(\tau_o) + \frac{2}{\tilde{\lambda}}\right] \left[\exp(-\tilde{\lambda}\Delta\tau) - 1\right]. \end{aligned} \quad (2)$$

Notice, the vibrating surface is now given by  $S(\tau) = \frac{\Gamma}{2\pi} \sin(2\pi\tau)$  where  $\Gamma = \frac{4\pi}{g} \frac{a}{T^2}$ .

## 3. The Mapping

The temporal variables  $\tau_1$  and  $\tau_0$  respectively are, the time at which the first collision occurs and the time at which the system initiates its dynamics. We define the particle-surface distance as  $D(\tau) = X(\tau) - S(\tau)$  and its derivative (relative velocity) denoted by  $\bar{\Omega}(\tau)$ .  $\Omega_o = V(\tau_o) - \Gamma \cos(2\pi\tau_o)$  is the relative velocity at  $\tau_o$  (the beginning of the motion), where  $X(\tau_o) = S(\tau_o)$ . Thus, for  $\tau_o \leq \tau \leq \tau_1$ , we have

$$\begin{aligned} D(\tau) &= \frac{\Gamma}{2\pi} [\sin(2\pi\tau_o) - \sin(2\pi\tau)] - \frac{2}{\tilde{\lambda}}\Delta\tau + \frac{1}{\tilde{\lambda}} \left[\Omega_o + \Gamma \cos(2\pi\tau_o) + \frac{2}{\tilde{\lambda}}\right] \left[1 - \exp(-\tilde{\lambda}\Delta\tau)\right], \\ \bar{\Omega}(\tau) &= -\Gamma \cos(2\pi\tau) - \frac{2}{\tilde{\lambda}} + \left[\Omega_o + \Gamma \cos(2\pi\tau_o) + \frac{2}{\tilde{\lambda}}\right] \exp(-\tilde{\lambda}\Delta\tau). \end{aligned} \quad (3)$$

We denote  $\Omega_1$  as the relative velocity just after the collision. We construct the dynamical mapping  $\mathcal{M} : (\tau_o, \Omega_o) \rightarrow (\tau_1, \Omega_1)$  by imposing at  $\tau_1$  the relative distance and the relative velocity to satisfy

$$\begin{aligned} D(\tau_1) &= 0, \\ \Omega_1 &= -\alpha \bar{\Omega}(\tau_1). \end{aligned} \quad (4)$$

Figure 1 schematically depicts the dynamics in the  $(\tau, \Omega)$ -space.

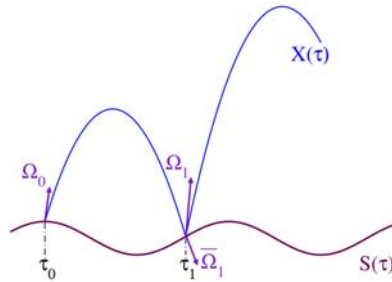


**Figure 1.** The dynamic of the system represented in the  $(\tau, \Omega)$  space.

#### 4. Fixed points and their stability

The mapping fixed points are defined by  $(\tau_*, \Omega_*)$ , satisfying the condition  $\Omega_1 = \Omega_o = \Omega_*$  and  $\tau_o = \tau_*$ ,  $\tau_1 = \tau_* + m$  (the integer  $m$  represents a platform cycle), then conditions given in Eqn.(4) become:

$$\begin{aligned} D(\tau_* + m) &= 0, \\ \Omega_* &= -\alpha \bar{\Omega}(\tau_* + m), \end{aligned} \quad (5)$$

yielding

$$\begin{aligned} \Gamma \cos(2\pi\tau_*) = \beta(\alpha, m, \tilde{\lambda}) &= \frac{2m}{(1+\alpha)} \frac{[1+\alpha \exp(-\tilde{\lambda}m)]}{[1-\exp(-\tilde{\lambda}m)]} - \frac{2}{\tilde{\lambda}}, \\ \Omega_* &= \frac{2\alpha}{(1+\alpha)} m. \end{aligned} \quad (6)$$

We discuss the stability of the fixed points by allowing small displacements around their neighborhood,  $\tau_o = \tau_* + \delta\tau_o$ ,  $\Omega_o = \Omega_* + \delta\Omega_o$ ,  $\tau_1 = \tau_* + m + \delta\tau_1$ ,  $\Omega_1 = \Omega_* + \delta\Omega_1$ . We define the convenient parameter  $\sigma = 2\pi^2 X(\tau_*) = \pi\Gamma \sin(2\pi\tau_*)$ . Linearizing Eqn.(4) in the standard fashion, we find

$$\begin{pmatrix} \delta\tau_1 \\ \delta\Omega_1 \end{pmatrix} = \begin{pmatrix} [1 - (1+\alpha)\sigma x] & \frac{1}{2}(1+\alpha)x \\ 2\alpha\sigma[(\alpha-z) - (1+\alpha)(1-\sigma x)] & \alpha[z - \sigma(1+\alpha)x] \end{pmatrix} \begin{pmatrix} \delta\tau_o \\ \delta\Omega_o \end{pmatrix}, \quad (7)$$

where  $\tilde{\lambda}mx = (1 - e^{-\tilde{\lambda}m})$  and  $z = \alpha e^{-\tilde{\lambda}m}$ .

The eigenvalues  $\chi_{\pm}$  of the monodromy matrix are computed by  $\chi_{\pm} = \left(\frac{\Sigma}{2}\right) \pm \sqrt{\left(\frac{\Sigma}{2}\right)^2 - \Pi}$ , where  $\Sigma$  (trace) and  $\Pi$  (determinant) are given respectively by

$$\begin{aligned} \Sigma &= (1+\alpha z) - (1+\alpha)^2 \sigma x, \\ \Pi &= \alpha z. \end{aligned} \quad (8)$$

Now, we analyze the nature of these solutions and their consequences on the stability of the dynamical mapping:

*4.0.1. Complex eigenvalues:*  $\left(\frac{\Sigma}{2}\right)^2 - \Pi < 0$ , yields the condition

$$\frac{(1 - \sqrt{\alpha z})^2}{(1+\alpha)^2 x} < \sigma < \frac{(1 + \sqrt{\alpha z})^2}{(1+\alpha)^2 x}. \quad (9)$$

A convenient parametric solution of the above condition is the linear interpolation  $\sigma(q) = \frac{[1+\alpha z - 2\sqrt{\alpha z}(1-2q)]}{(1+\alpha)^2 x}$  with  $0 \leq q \leq 1$ . It follows: (i) if  $0 \leq q \leq 1/2$ , then  $\Sigma = 2\Re \chi_{\pm} > 0$ ; (ii) if  $1/2 \leq q \leq 1$ , then  $\Sigma = 2\Re \chi_{\pm} < 0$ .

*4.0.2. Real eigenvalues:*  $\left(\frac{\Sigma}{2}\right)^2 - \Pi > 0$ , yields: (i)  $\sigma < \frac{(1-\alpha z)^2}{(1+\alpha)^2 x}$  and the solution are  $\chi_{\pm} > 0$ ; (ii)  $\sigma > \frac{(1+\alpha z)^2}{(1+\alpha)^2 x}$  and the solutions are  $\chi_{\pm} < 0$ .

We compact our results defining:  $\sigma_o = \frac{(1+\alpha z)}{(1+\alpha)^2 x}$ ,  $\Delta = \frac{2\sqrt{\alpha z}}{(1+\alpha)^2 x}$  and  $\sigma_o^{\pm} = \sigma_o \pm \Delta$ . The table below displays the several eigenvalues regimes, for a given value of  $\sigma$ :

$\sigma < \sigma_o^-$	$\sigma_o^- < \sigma < \sigma_o$	$\sigma_o < \sigma < \sigma_o^+$	$\sigma > \sigma_o^+$
Real: $\chi_{\pm} > 0$	Complex: $\Re \chi_{\pm} > 0$	Complex: $\Re \chi_{\pm} < 0$	Real: $\chi_{\pm} < 0$

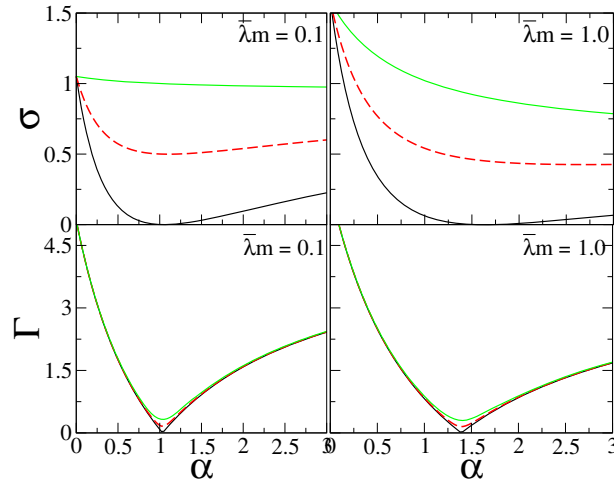


**Figure 2.** We plot  $\sigma$  and  $\Gamma$  versus  $\alpha$ , for  $m = 5$  and  $\lambda = 2 \times 10^{-2}, 2 \times 10^{-1}$ . Values of  $\sigma$  above the continuous green line and below the continuous black line define real eigenvalues. The region between the continuous-black-line and the continuous-green-line define the complex eigenvalues.

Notice that, for given  $\tilde{\lambda}$  and  $m$ ,  $\Gamma$  is computed, from Eqn. (6) as

$$\Gamma = \sqrt{\left(\frac{\sigma}{\pi}\right)^2 + \beta^2}. \quad (10)$$

Figure 2 displays  $\sigma$  and  $\Gamma$  as functions of the restitution coefficient  $\alpha$ , for  $m = 5$  and for  $\tilde{\lambda}$  equal to  $2 \times 10^{-2}$  and  $2 \times 10^{-1}$ . For the  $\sigma$ 's values above the continuous green line eigenvalues are real and negative, below the continuous black line the eigenvalues are real and positive. For values in between green and black line the eigenvalues are complex.

Finally, we analyze the stability of the system according to the eigenvalues' modules:

Complex $\chi$	$ \chi_{\pm}  = \alpha e^{-\tilde{\lambda}m/2} < 1$ , stable/focus $ \chi_{\pm}  = \alpha e^{-\tilde{\lambda}m/2} > 1$ , unstable/source	Depending on $\alpha, \tilde{\lambda}$ and $m$
Real $\chi$	$ \chi_{\pm}  < 1$ , stable/node $ \chi_-  < 1 <  \chi_+ $ , hyperbolic/saddle $ \chi_{\pm}  > 1$ , unstable/node	Depending on $\Gamma, \alpha, \tilde{\lambda}$ and $m$

## 5. Global aspects of the dynamics

### 5.1. The phase space volume

Both variables  $\Omega$  and  $\Delta\tau$  will remain bounded, as long as the parameters  $\alpha$  and  $\tilde{\lambda}$  are appropriately chosen. In order to estimate the upper bounds  $\Omega_{max}$  and  $\Delta\tau_{max}$ , we consider the reduced phase space, where the time variable compact (see just above eqn.5). A rough upper bound can be derived from Eqns.(3-4),

$$\begin{aligned} \Omega_1 &\leq \alpha \left\{ \Gamma + \frac{2}{\tilde{\lambda}} - \left[ \Omega_o + \Gamma + \frac{2}{\tilde{\lambda}} \right] \exp(-\tilde{\lambda}\Delta\tau) \right\}, \\ D(\tau) &\leq \frac{\Gamma}{\pi} - \frac{2}{\tilde{\lambda}}\Delta\tau + \frac{1}{\tilde{\lambda}} \left[ \Omega_o + \Gamma + \frac{2}{\tilde{\lambda}} \right] \left[ 1 - \exp(-\tilde{\lambda}\Delta\tau) \right]. \end{aligned} \quad (11)$$

We maximize  $\Omega_0 = \Omega_1 = \Omega_{max}$ , from Eqn. (6) yielding  $\Gamma = \frac{2}{\tilde{\lambda}} \left[ \frac{\tilde{\lambda}m}{(1+\alpha)} \frac{(1-\alpha e^{-\tilde{\lambda}m})}{(1-e^{-\tilde{\lambda}m})} - 1 \right]$  and

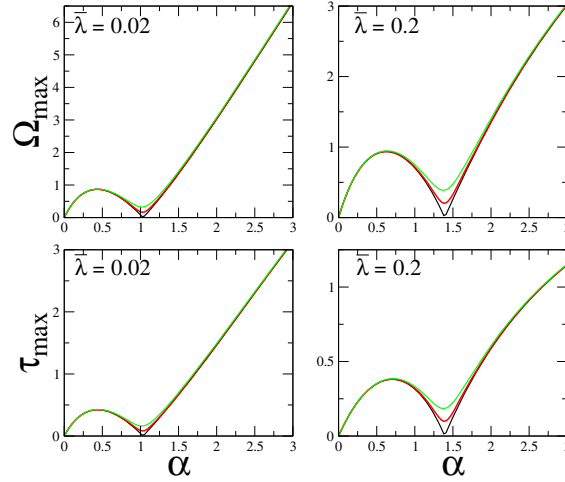


**Figure 3.** The maximum values for both the relative velocity and time versus the restitution coefficient, for  $m = 5$  and two values of the damping force.

by linearizing the latter, we obtain  $m_{max} = \frac{(1+\alpha)\Gamma/2}{1+\frac{\tilde{\lambda}}{2}(1+\alpha)\Gamma}$ , thus

$$\Omega_{max} = \frac{\alpha\Gamma}{1+\frac{\tilde{\lambda}}{2}(1+\alpha)\Gamma} \quad , \quad \Delta\tau_{max} = \frac{1}{\tilde{\lambda}} \ln \left( \frac{1+\frac{\tilde{\lambda}}{2}(\Omega_{max}+\Gamma)}{1+\frac{\tilde{\lambda}}{2}\Gamma} \right). \quad (12)$$

In Figure 3 we plot the maximum values of both the relative velocity and the time as a function of the restitution coefficient. Both plots feature a critical value  $\alpha_c$  ( $\approx 1$  or  $1.5$ ,  $\tilde{\lambda}$  dependence). For  $\alpha < \alpha_c$  the dynamical variables become bounded.

### 5.2. Absorbing and transmitting regions

Following [7], one cycle of the vibrating surface can be decomposed into a transmitting and an absorbing region, according to whether or not long flights are allowed. For any take-off time  $0 < \tau_0 < 1$ , we define  $(\theta, \Omega_A)$  at the point where the collision occurs with relative velocity zero; and from eqn.(3) we obtain

$$\begin{aligned} \frac{\Gamma}{2\pi} [\sin(2\pi\tau_0) - \sin(2\pi\theta)] - \frac{2}{\tilde{\lambda}}(\theta - \tau_0) + \frac{1}{\tilde{\lambda}} \left[ \Omega_A + \Gamma \cos(2\pi\tau_0) + \frac{2}{\tilde{\lambda}} \right] [1 - e^{-\tilde{\lambda}(\theta-\tau_0)}] &= 0, \\ -\Gamma \cos(2\pi\theta) - \frac{2}{\tilde{\lambda}} + \left[ \Omega_A + \Gamma \cos(2\pi\tau_0) + \frac{2}{\tilde{\lambda}} \right] e^{-\tilde{\lambda}(\theta-\tau_0)} &= 0. \end{aligned} \quad (13)$$

By linearizing and considering  $\Gamma \gg \tilde{\lambda}$ , we obtain approximate expressions for  $\Omega_A$  and  $\theta$

$$\Omega_A/\Gamma = e^{\tilde{\lambda}(\theta-\tau_0)} \cos(2\pi\theta) - \cos(2\pi\tau_0). \quad (14)$$

$$\{\sin(2\pi\tau_0) - \sin(2\pi\theta)\} + 2\pi \left\{ \cos(2\pi\theta) - \tilde{\lambda} [\sin(2\pi\tau_0) - \sin(2\pi\theta)] \right\} (\theta - \tau_0) + \tilde{\lambda} \pi \cos(2\pi\theta) (\theta - \tau_0)^2 = 0. \quad (15)$$

When  $\Omega_0 < \Omega_A$  (absorbing region) the particle rides on the membrane allowing some small bouncing (chattering) or simply stick to the membrane (locking) until the velocity is reverse and  $\Omega_A > \Omega_o$ . In the latter case, namely  $\Omega_o > \Omega_A$  (transmitting region) the ball is launched with a strong impulse.

## 6. Conclusions

We presented a model strictly derived from the equation of motion of a ball colliding against a vibrating surface, influenced by both gravitational and a Stokes-like damping forces. We constructed the associated mapping governing the system's dynamical motion. We computed the mapping fixed points and discussed its stability. The bounded motion regime exist even for  $\alpha > 1$  and the complexity of the absorbing-transmitting region depends on the dissipative constant  $\tilde{\lambda}$ . We emphasize that our model rescues well known results in the limit  $\lambda = 0$ , as in [7].

In order to obtain a quantitative picture of the many dynamical regimes in parameter space we have ongoing numerical calculations. Our results can be applied to a variety of areas. In particular, granular flows gives rise to a variety of phenomena such as convection, surface excitation and fluidization. In all cases the character of collision between a grain and a wall of the container strongly affects the dynamical behavior of such dissipative media [3]. Another interesting issue refers to the study of the dissipative effects on regular or chaotic trajectories [8], including relativistic effects [2].

## Acknowledgments

The authors would like to thank the support of the Goiás Research Foundation - FAPEG.

## References

- [1] Pustil'nikov L D 1983 Theor Math Phys **57** 1035-1038
- [2] Pinto Rafael S and Letelier Patricio S 2011 Phys Lett A **375** 3273-3278
- [3] Falcon E, Laroche C, Fauve S and Coste C 1998 Eur Phys J B **3** 45-47
- [4] Lieberman M A and Lichtenberg A J 1971 Phys Rev A **5** 1852-1866
- [5] Fermi E 1949 Phys Rev **75** 1169-1174
- [6] Oliveira Diego F M and Leonel Edson 2011 New Journal of Physics **13** 123012
- [7] Luck J M and Mehta Anita 1993 Phys. Rev. E **48**(5) 3988-3997
- [8] Jousseph C A , Kruger T S , Manchein C, Lopes S R , Beims M.W. 2016 Physica A **456** 68-74